Ⓔ

A PLANETARY COMPANION TO γ CEPHEI A

ARTIE P. HATZES

Thüringer Landessternwarte, D-07778 Tautenburg, Germany;
artie@jupiter.tls-tautenburg.de

WILLIAM D. COCHRAN, MICHAEL ENDL, BARBARA MCARTHUR, AND DIANE B. PAULSON

McDonald Observatory and Astronomy Department, University of Texas at Austin, Austin, TX 78712;
wdc@astro.as.utexas.edu, mike@astro.as.utexas.edu, mca@astro.as.utexas.edu, apodis@astro.as.utexas.edu

GORDON A. H. WALKER

Physics and Astronomy Department, University of British Columbia, Vancouver, BC V6T 1Z4, Canada;
walker@astro.ubc.ca

BRUCE CAMPBELL

BTEC Enterprises Limited

AND

STEPHENSON YANG

Department of Physics and Astronomy, University of Victoria, Victoria, BC V8W 3P6, Canada;
yang@uvastro.phys.uvic.ca

Received 2003 April 30; accepted 2003 August 22

ABSTRACT

We report on the detection of a planetary companion in orbit around the primary star of the binary system γ Cephei. High-precision radial velocity measurements using four independent data sets spanning the time interval 1981–2002 reveal long-lived residual radial velocity variations superposed on the binary orbit that are coherent in phase and amplitude with a period or 2.48 yr (906 days) and a semiamplitude of 27.5 m s^{-1}. We performed a careful analysis of our Ca II H and K S-index measurements, spectral line bisectors, and *Hipparcos* photometry. We found no significant variations in these quantities with the 906 day period. We also reanalyzed the Ca II λ8662 measurements of Walker et al., which showed possible periodic variations with the "planet" period when first published. This analysis shows that periodic Ca II equivalent width variations were only present during 1986.5–1992 and absent during 1981–1986.5. Furthermore, a refined period for the Ca II λ8662 variations is 2.14 yr, significantly less than the residual radial velocity period. The most likely explanation of the residual radial velocity variations is a planetary-mass companion with $M \sin i = 1.7 M_{\rm J}$ and an orbital semimajor axis of $a_2 = 2.13$ AU. This supports the planet hypothesis for the residual radial velocity variations for γ Cep first suggested by Walker et al. With an estimated binary orbital period of 57 yr, γ Cep is the shortest period binary system in which an extrasolar planet has been found. This system may provide insights into the relationship between planetary and binary star formation.

Subject headings: planetary systems — stars: individual (γ Cephei A) — techniques: radial velocities

On-line material: color figures

1. INTRODUCTION

The first high-precision radial velocity (RV) survey for planetary companions to nearby stars was conducted with the use of a hydrogen fluoride (HF) gas absorption cell on the Canada-France-Hawaii Telescope (CFHT; Campbell & Walker 1979; Walker et al. 1995). The γ Cephei system (HR 8974 = HD 222404 = HIP 116727) was one of 16 stars on the observing list of this program. Campbell, Walker, & Yang (1988) reported that two of the stars on the observing list (γ Cephei and χ^1 Orionis) were previously unknown single-lined spectroscopic binaries. In the case of γ Cephei, Campbell et al. (1988) found evidence for RV "bumps" superposed on the large-amplitude binary motion. The residuals after removing the binary orbit yielded a period of about 2.7 yr and a velocity semiamplitude of about 25 m s^{-1}. The authors examined several possible causes of the observed RV variability and finally concluded that the system had a "probable third body." If substantiated, this would have been the first detection of an extrasolar planetary system. However, Bohlender et al. (1992) classi-

fied γ Cep as a K0 III star, raising the possibility that the observed RV variations were due to the recently discovered (Walker et al. 1989; Hatzes & Cochran 1993) long-period RV variability of most K giants. A detailed analysis of the CFHT RV data on γ Cep by Walker et al. (1992) showed a clear low-amplitude (27 m s^{-1}) signal with a 2.52 yr period superposed on the binary orbital motion of indeterminate period. They also found evidence of a possible variation of the Ca II λ8662 emission line index with the same 2.5 yr period, leading them to conclude that the observed low-amplitude RV variation was most likely due to K-giant variability at the period of the stellar rotation.

Here we present new high-precision RV data on the γ Cephei system obtained from McDonald Observatory. When combined with the CFHT data, we show that the 2.5 yr low-amplitude RV variability of γ Cep has remained constant for over 20 yr. A simultaneous orbital solution for both the binary star and the 2.5 yr low-amplitude variability is computed. We demonstrate that there is no correlation between the low-amplitude RV variations and the Mount Wilson Ca II S-index, nor is there any indication of

photospheric absorption line profile variability. These results, combined with the current best classification of γ Cep as a K1 IV star (Fuhrmann 2003), all indicate that the preferred interpretation of the data is that γ Cep A has a planetary-mass companion in a 2.5 yr period orbit.

2. THE RADIAL VELOCITY DATA SETS

We consider four independent sets of high-precision RV data for γ Cephei, covering the interval from 1981 through 2002. The first of these is from the CFHT survey (Campbell et al. 1988; Walker et al. 1995), with the velocities taken from Table 1 of Walker et al. (1992). All of the other data were from the McDonald Observatory Planetary Search (MOPS) program (Cochran & Hatzes 2003). Phase I of the MOPS program used the telluric O_2 lines near 6300 Å as the velocity metric, a technique suggested by Griffin & Griffin (1973). A single order of the 2.7 m coudé spectrometer "6 foot camera" with the echelle grating was isolated onto a Texas Instruments (TI) 800×800 CCD at $R = 210,000$. This system gave 15–20 m s^{-1} precision on stars down to about $V = 6$ but suffered from systematic velocity errors, most likely due to prevailing atmospheric winds. In 1992, the program switched to a temperature-stabilized I_2 cell (Koch & Wöhl 1984; Libbrecht 1988) as the velocity metric for phase II of the MOPS ($R = 210,000$ for these data as well). This eliminated the systematic errors and gave a routine RV precision of 15 m s^{-1}. This precision was limited by the 9.6 Å bandpass of the spectrum and by the poor charge transfer and readout properties of the TI CCD. To solve these problems and to achieve substantially improved precision, we began phase III of the RV program in 1998 July, using the I_2 cell with the newly installed 2dcoudé cross-dispersed echelle spectrograph (Tull et al. 1995). This instrument, when used with a Tektronix 2048×2048 detector, provides a nominal wavelength coverage of 3600 Å–1 μm at a resolving power of $R = 60,000$. The Tektronix CCD also had significantly better charge transfer and readout properties than the TI device. The complete spectral coverage of 2dcoudé gives us two advantages: first, we can utilize the full reference spectrum of the I_2 cell for the RV determination, and second, we can simultaneously determine the stellar chromospheric emission in the cores of the Ca II H and K lines to use as stellar chromospheric activity indicators. We will discuss in detail the question of whether there is a correlation between the RV results and the activity indices for γ Cep in § 4.

To extract the RV information from the I_2 self-calibrated spectra taken during phase III, we employed our AUSTRAL RV code, which uses a maximum entropy method deconvolution in order to obtain a more highly resolved stellar template spectrum and several reconstruction algorithms, which model the shape and symmetry of the instrumental profile (IP) at the time of observation. A detailed description of the AUSTRAL code can be found in Endl, Kürster, & Els (2000). The algorithm follows, in general, the modeling idea first outlined by Butler et. al. (1996) and the IP reconstruction techniques by Valenti, Butler, & Marcy (1995). Using the 2dcoudé spectrometer in I_2 cell self-calibration mode and the AUSTRAL code for the analysis, we obtain a long-term RV precision of 5–15 m s^{-1} on a routine basis for stars down to a magnitude of $V = 9.0$.

All of the MOPS data from phases I, II, and III are given in Tables 1–3. The uncertainties quoted there for phase II

TABLE 1
McDonald Observatory Phase I Radial Velocities

JD-2400000.0	Radial Velocity (m s^{-1})	σ (m s^{-1})
47368.9657............	550.0	19.0
47369.9300............	570.8	19.0
47369.9346............	572.0	19.0
47405.9338............	500.8	19.0
47430.7110............	530.6	19.0
47430.7141............	520.5	19.0
47459.7569............	495.2	19.0
47460.7559............	488.8	19.0
47495.7539............	416.4	19.0
47495.7597............	416.3	19.0
47496.7046............	437.9	19.0
47516.6665............	440.0	19.0
47517.6587............	416.1	19.0
47551.6057............	397.0	19.0
47551.6101............	391.9	19.0
47582.5740............	359.1	19.0
47696.9685............	274.9	19.0
47762.9403............	220.3	19.0
47785.9286............	152.9	19.0
47785.9319............	157.6	19.0
47786.8176............	171.1	19.0
47786.8210............	166.3	19.0
47813.7499............	133.5	19.0
47848.6803............	102.9	19.0
47879.6591............	70.0	19.0
47880.7112............	67.7	19.0
47895.6235............	72.0	19.0
48145.8981............	−112.5	19.0
48145.9039............	−112.2	19.0
48146.8217............	−89.4	19.0
48176.8457............	−143.4	19.0
48176.8513............	−153.7	19.0
48198.8661............	−182.7	19.0
48227.7128............	−178.0	19.0
48523.8192............	−277.6	19.0
48523.8241............	−278.0	19.0
48854.9066............	−390.1	19.0
48903.8517............	−426.3	19.0
49260.7901............	−327.9	19.0
49260.7946............	−325.2	19.0
49649.7368............	−235.8	19.0
49649.7390............	−243.4	19.0
49649.7411............	−234.7	19.0

and III data are the "internal" errors, as represented by the rms of the individual spectral chunks about the mean value. We regard these as a lower limit on the actual uncertainties, since these values do not include the effects of any residual systematic errors that may be present. It is difficult to estimate internal errors for the phase I data because these are not analyzed in "chunks" like the phase II and III measurements. Phase I observations of a constant star (τ Cet) show an rms scatter of 23 m s^{-1}. The rms scatter of the phase I measurements about the final orbital solution is 17.4 m s^{-1}. We list a slightly higher value of 19 m s^{-1} as the "error" of the phase I measurements in Table 1. This error was the most reasonable error to assign, based on χ^2 tests of the data, and was the value assumed for the phase I measurements in the final orbital solutions. The true error for an individual phase I measurement is almost surely higher as a result of different signal-to-noise ratios of individual spectra

TABLE 2
McDonald Observatory Phase II Radial Velocities

JD−2400000.0	Radial Velocity (m s⁻¹)	σ (m s⁻¹)
48177.8696....................	35.39	33.09
48177.8773....................	29.94	23.82
48200.8311....................	27.72	13.42
48224.7008....................	53.95	11.53
48259.6020....................	42.85	13.09
48484.8393....................	−37.21	14.00
48524.8304....................	−93.10	17.55
48555.7939....................	−105.15	12.07
48555.8038....................	−116.01	9.08
48607.7638....................	−138.18	13.85
48644.6465....................	−137.70	16.41
48824.9547....................	−204.50	20.26
48824.9609....................	−192.72	24.48
48852.9733....................	−209.83	20.32
48853.9149....................	−212.64	18.76
48882.8273....................	−205.27	12.96
48901.7912....................	−225.14	10.72
48902.7764....................	−235.24	18.78
48943.7443....................	−246.38	15.91
48971.6571....................	−238.61	18.23
48973.6189....................	−205.78	19.50
49020.6401....................	−218.97	13.72
49220.9732....................	−167.29	33.39
49258.8484....................	−132.89	17.28
49286.7903....................	−181.63	15.92
49352.6804....................	−119.99	18.05
49380.5871....................	−97.26	19.21
49400.5656....................	−116.95	17.10
49587.8845....................	−68.05	16.10
49587.8907....................	−61.08	17.55
49615.8899....................	−72.07	14.53
49647.8128....................	−73.35	10.00
49670.7118....................	−28.25	8.18
49703.6783....................	−35.81	12.4
49734.5877....................	−28.56	15.26
49769.5639....................	−22.20	11.46
49917.9326....................	87.22	12.25
49946.9247....................	103.39	36.52
49963.8567....................	135.27	20.53
49993.8304....................	127.05	16.89
50093.6243....................	188.90	8.42
50124.6006....................	222.54	8.77
50292.8908....................	351.62	13.65
50354.8007....................	389.66	9.85
50409.7363....................	394.82	14.13
50480.6530....................	420.67	15.16
50700.8995....................	556.24	16.33
50768.8008....................	575.22	14.58
50834.6049....................	650.27	12.11

TABLE 3
McDonald Observatory Phase III Radial Velocities

JD−2400000.0	Radial Velocity (m s⁻¹)	σ (m s⁻¹)
51010.8960....................	−583.71	7.55
51010.9008....................	−578.23	7.61
51065.8469....................	−555.03	7.60
51152.6120....................	−471.87	8.93
51212.5924....................	−420.20	8.78
51212.5964....................	−422.45	8.63
51417.9144....................	−328.56	7.93
51451.8399....................	−306.73	8.01
51503.6547....................	−290.01	7.93
51503.6584....................	−293.29	7.93
51503.6617....................	−294.87	7.76
51530.7206....................	−280.93	8.42
51556.6279....................	−266.48	8.48
51750.9434....................	−146.12	7.14
51775.8747....................	−114.43	7.88
51811.8113....................	−83.07	7.64
51919.5884....................	−13.88	7.89
51946.7192....................	13.03	9.18
52117.9545....................	131.98	7.77
52221.8443....................	164.75	8.37
52328.6118....................	194.18	7.82
52472.9542....................	260.48	7.64
52472.9575....................	258.52	8.06
52473.9522....................	248.31	7.68
52473.9553....................	246.10	7.77
52492.8857....................	250.44	7.62
52492.8876....................	241.13	7.43
52493.8549....................	256.65	7.93
52493.8567....................	244.26	7.66
52494.9286....................	257.24	7.66
52494.9302....................	264.18	7.76
52495.9152....................	255.16	7.61
52538.8445....................	284.82	8.07
52538.8465....................	278.53	7.97
52576.7817....................	306.18	7.90
52599.6345....................	331.50	8.28
52599.6370....................	314.88	8.29
52621.7124....................	323.18	8.17
52621.7148....................	324.99	8.41

after subtraction of the velocity variations due to the binary companion (see below). The top panel is only for the CFHT data. The middle panel is for the CFHT+McDonald data, excluding the phase III data. The bottom panel is the periodogram for all of the RV measurements. The increase in power at a period of ≈2.5 yr with the addition of each data set is the first indication that these residual RV variations are long-lived and coherent. (The false-alarm probability [FAP] of the peak for the full data set is ≈10^{-20}).

3. ORBITAL SOLUTIONS

The program GaussFit (Jefferys, Fitzpatrick, & McArthur 1988; McArthur, Jefferys, & McCartney 1994) was used to fit simultaneously all orbital parameters for both the stellar and the presumed substellar companion, using nonlinear least-squares with robust estimation. Because each instrument produces relative RVs with their own arbitrary zero point, the individual velocity offsets were a free parameter in the least-squares solution. Table 4 gives
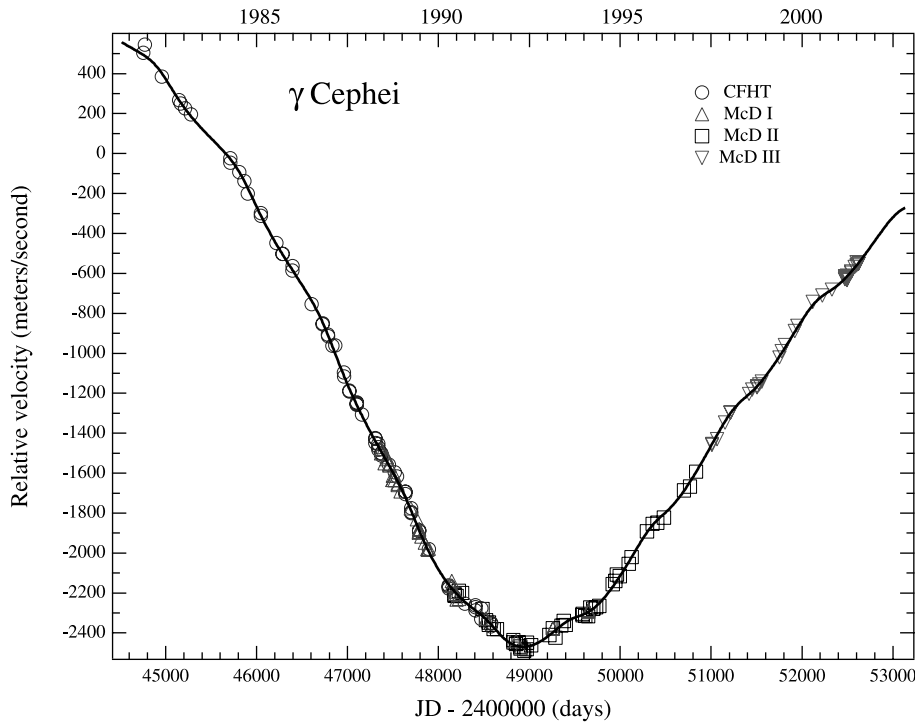
and systematic errors due to wind and temperature and pressure changes in the Earth's atmosphere.

The RV measurements for all data sets are shown in Figure 1. A different velocity offset (see below) had to be applied to each data set so that they would all have the same zero point. One can clearly see that the "wiggles" superposed on the binary variations, which were first reported by Walker et al. (1992), are still present in the final data set (phase III) taken 20 yr later.

Figure 2 shows a sequence of Lomb-Scargle periodograms (Lomb 1976; Scargle 1982) of the RV measurements

Fig. 1.—Combined (planet+stellar) orbital solution to all RV data sets for γ Cep. Circles represent the CFHT measurements of Walker et al. (1992). All other symbols represent data taken at McDonald Observatory. Triangles represent measurements using telluric O_2 as the reference (phase I), squares represent measurements using an iodine absorption cell (phase II), and inverted triangles represent I_2 measurements, but with the large wavelength coverage 2dcoudé spectrograph (phase III).

the velocity offsets of the different data sets. Subtracting these velocity offsets from an individual data set will place them all on the same RV scale. The line in Figure 1 shows the combined orbital solution to γ Cep. Figure 3 shows the "planet-only" orbital solution after subtracting the contribution of the binary orbit to the RV measurements.

Table 5 lists the orbital parameters for the the stellar companion. The errors listed are the correlated errors that are

produced by GaussFit. The largest error occurs in the period, since our observations span about 20 yr, or about one-third of the binary orbit. Note that the reduced χ^2 of the "binary-only" orbital solution is rather large (4.36), indicating the presence of additional RV variations.

Griffin, Carquillat, & Ginestet (2002) presented an orbital solution for the stellar companion to γ Cep. They combined RV measurements spanning over 100 yr taken at five observatories. These measurements included the CFHT data, as well as some of our McDonald Observatory measurements (read from an enlarged copy of a published graph!). The parameters of their orbital solution are also listed in Table 5. In spite of the more limited time span of our observations, our orbital solution agrees quite well with the Griffin et al. orbit.

Table 6 lists the GaussFit orbital parameters for the substellar companion. Also listed is the rms scatter of the individual data sets about the combined orbital solution. The period of 2.48 yr and semiamplitude of 27.5 m s^{-1} are consistent with the values found by Walker et al. (1992), using only the CFHT data set. Note that the reduced χ^2 is
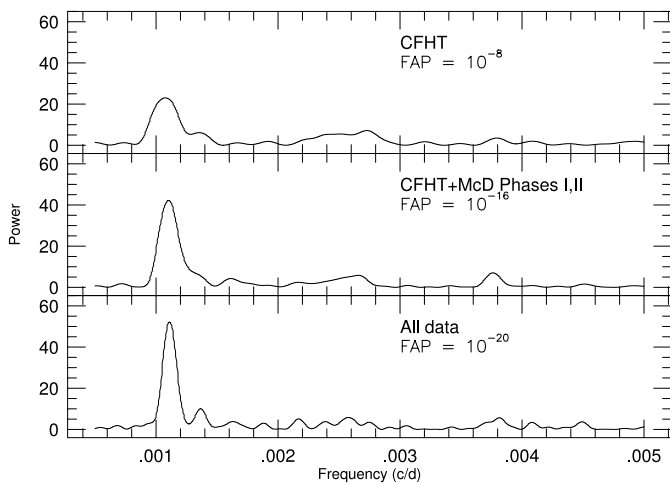
Fig. 2.—Lomb-Scargle periodogram of the combined RV measurements for γ Cep after removal of the RV variations due to the stellar companion. *Top*: CFHT data alone. *Middle*: Periodogram of the combined CHFT+McDonald phase I and II data. *Bottom*: Periodogram of all measurements. The FAP for the peak in each periodogram is shown in each panel. This was computed using the equation given in Scargle (1982).

TABLE 4
VELOCITY OFFSETS FOR THE DATA SETS

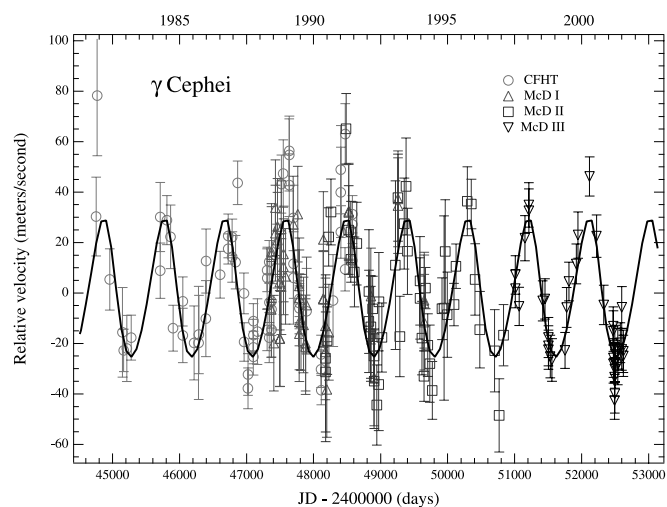| Data Set	Velocity Offset (m s^{-1})
CFHT.........................	1294.6 ± 108
McD phase I	2232.3 ± 108
McD phase II..............	2040.8 ± 110
McD phase III	864.7 ± 108

FIG. 3.—Orbital solution for the planet (*line*) and the residual velocity measurements of the four data sets after subtracting the contribution due to the binary companion (*points*). [*See the electronic edition of the Journal for a color version of this figure.*]

significantly lower ($\chi^2 = 1.47$) when including the planet in the orbital solution. Fuhrmann (2003) estimates the primary mass of γ Cep as $M = 1.59 \pm 0.12~M_\odot$. This results in a planetary mass of $M_p \sin i = 1.7 \pm 0.4 M_J$ and an orbital semimajor axis of 2.13 AU.

Figure 4 shows the phase diagram of the individual data sets. The phase, amplitude, and overall shape of the RV curves hold up remarkably well over a 20 yr time span, again evidence for long-lived and coherent variations that are consistent with the presence of a planetary companion.

4. THE NATURE OF THE RV VARIATIONS

The question naturally arises as to whether some phenomena instrinsic to the star (spots, convective shifts, pulsations) are responsible for the 2.48 yr period. After all, γ Cep is most likely a subgiant (see below), a class of stars for which magnetic activity, surface structure, convection, and pulsations are poorly known. Moreover, Walker et al. (1992) did find evidence for weak periodic variations in the equivalent width (EW) of the Ca II $\lambda8662$ line with the same period as the planet. In spite of the intrinsic variability of giant stars, planetary companions have been found around other giant stars (Frink et al 2002; Setiawan et al. 2003) and one subgiant (Butler et al. 2001). So the existence of planets around giant evolved stars is not an unreasonable

hypothesis. Before concluding that the planet hypothesis is the most likely explanation for the residual RV variations, we must demonstrate that γ Cep does not exhibit any significant variations with the planet period in other quantities. Here we examine whether γ Cep also has spectral and photometric variations.

4.1. *Bisector Analysis*

The spectral line shapes can also provide evidence in support of the planetary hypothesis. Surface features (Hatzes 2002) or nonradial pulsations (Hatzes 1996; Brown et al. 1998) should produce changes in the spectral line shapes with the same period as the RV variations. A convenient means of measuring the asymmetry of a spectral line is the line bisector, or the line segments connecting the midpoints of the spectral line from the core to the continuum. Line bisector studies have been used to establish the planetary nature of 51 Peg (Hatzes, Cochran, & Johns-Krull 1997; Hatzes, Cochran, & Bakker 1998a, 1998b) and the starspot nature of the planet-like RV variations in HD 166435 (Queloz et al. 2001).

The McDonald Observatory phase I observations taken in the 6300 Å region provide an excellent data set for studying possible line profile variations in γ Cep. The data have very high spectral resolution ($R = 210,000$), and there are several strong spectral lines that were velocity-shifted clear of the telluric features because of the Earth's barycentric velocity. The Fe I $\lambda6301.5$ feature was free of telluric lines over the entire data set, Fe I $\lambda6297.8$ for 30 observations, and Fe I $\lambda6302.5$ for eight observations. Both the bisector velocity span and curvature were measured for these lines. The velocity span is defined as the velocity difference between two arbitrary points on the line bisector, while the curvature is the difference between the velocity span of the top half of the bisector minus the velocity span of the bottom half of the bisector.

A fifth-order polynomial was fitted to each measured line bisector and the velocity span points taken at 0.4 and 0.8 of the continuum. (In measuring the line bisector, one should avoid both the core and the continuum, where the errors in the bisector measurement become large.) The additional point required for the curvature measurements was taken at 0.6 of the continuum value. The mean value of the bisector span and curvature for each line was then subtracted from the individual measurements, and the residual span and velocity measurements were then averaged, weighted by the rms scatter of the bisector measurements for each spectral line.

TABLE 5
BINARY ORBITAL ELEMENTS FOR γ CEP

Element	This Work	Griffin et al. 2002
Period (days)	20750.6579 ± 1568.6	24135 ± 349
T (JD)	248429.03 ± 27.0	248625 ± 210
Eccentricity	0.361 ± 0.023	0.389 ± 0.017
ω (deg)	158.76 ± 1.2	166 ± 7
K1 (km s^{-1})	1.82 ± 0.049	2.04 ± 0.10
$f(m)$ ($M_\odot$)	0.0106 ± 0.0012	0.0166 ± 0.0025
Semimajor axis (AU)	18.5 ± 1.1	20.3 ± 0.7
Reduced χ^2 (without planet)	4.36	$\ldots$

TABLE 6
ORBITAL ELEMENTS FOR PLANET AROUND γ CEP

Element	Value
Period (days)...........................	905.574 ± 3.08
T (JD)	253121.925 ± 66.9
Eccentricity............................	0.12 ± 0.05
ω (deg)....................................	49.6 ± 25.6
K1 (m s^{-1}).............................	27.50 ± 1.5
$f(m)$ ($M_\odot$)............................	$(1.90 \pm 0.3) \times 10^{-9}$
Semimajor axis (AU).............	2.13 ± 0.05
Reduced χ^2	1.47
σ_{CFHT} (m s^{-1})........................	15.3
$\sigma_{Phase I}$ (m s^{-1})........................	17.4
$\sigma_{Phase II}$ (m s^{-1})........................	15.8
$\sigma_{Phase III}$ (m s^{-1})......................	8.2

Figure 5 shows the phase-binned averages ($\Delta\phi \approx 0.05$) of the bisector span and curvature variations for γ Cep, phased to the planet orbital period. The short-dashed horizontal line gives the zero-point reference, and the long-dashed lines show the velocity extrema of the residual RV variations due to the planetary companion. There are no obvious phase variations of the bisector quantities with the planet period. The least-squares sine fit to the bisector quantities, assuming a period of 906 days, yields amplitudes of 4.8 ± 4.4 and 2.4 ± 4.5 m s^{-1} for the bisector and span variations, respec-

tively. These amplitudes are consistent and are significantly less than the observed 27 m s^{-1} RV variations of the planet.

The McDonald phase I data had the largest errors of all the data sets, and the phase variations of these show the least evidence for the 906 day period (Fig. 4). One could argue that there are no residual RV variations with which to correlate to the bisector measurements. However, the phase I data are still consistent with the presence of the planet signal. Not only is this signal present in the phase I and II data alone, but the power increases by almost a factor of 2 over the individual periodograms when the two data sets are combined. Although not obvious to the eye, the 906 day period is still present in the phase I data. On the other hand, the averaged, phase-binned bisector measurements have variations significantly less than the 906 day RV amplitude, and we believe that this adds additional evidence (along with the photometric and Ca II analysis presented below) in support of the planet hypothesis. *If* the bisector variations had scatter comparable to the RV amplitude, then one could at least make a plausible argument in favor of possible bisector variability. Figure 5 excludes that.

4.2. *Photometric Variations*

The *Hipparcos* mission (Perryman et al. 1997) took high-precision photometric measurements of γ Cep contemporaneously with the measurements used for our RV study. If cool spots on the stellar surface or some form of stellar
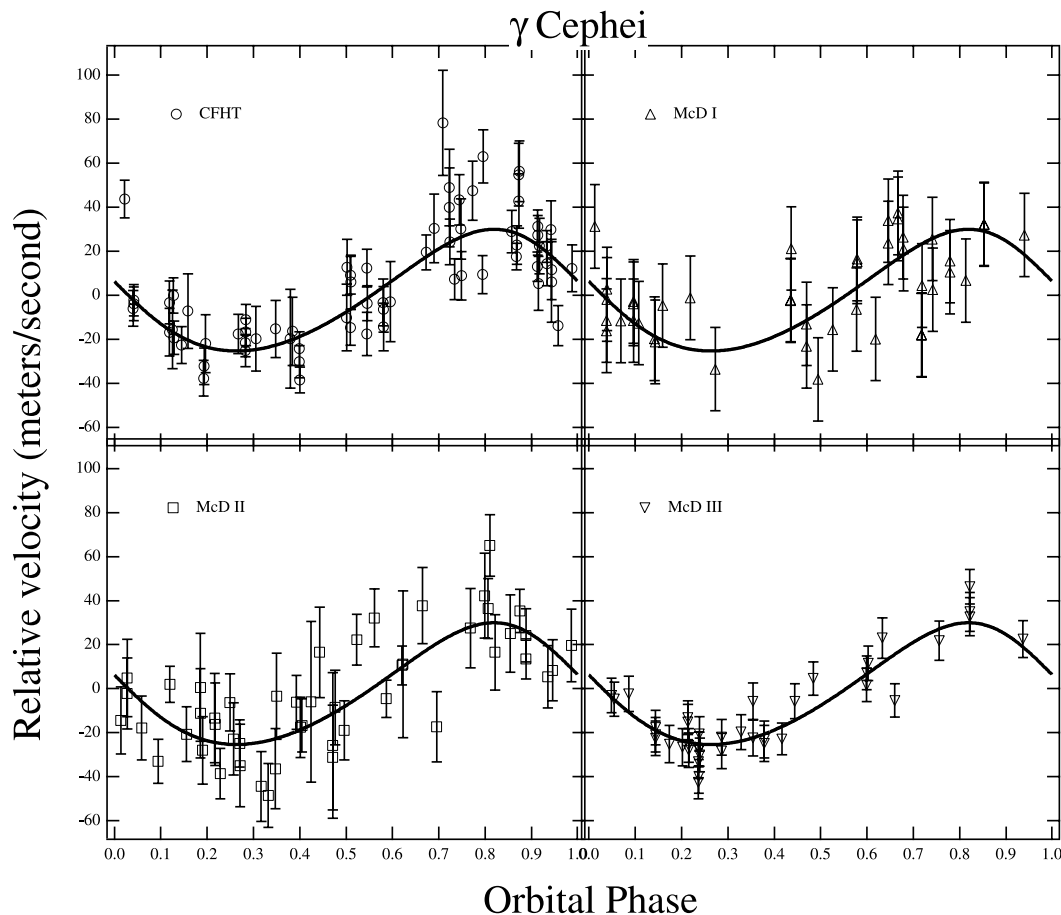

FIG. 4.—Phased residual RV measurements from CFHT and McDonald phase I–III compared to the planet orbital solution (*line*). [*See the electronic edition of the Journal for a color version of this figure.*]
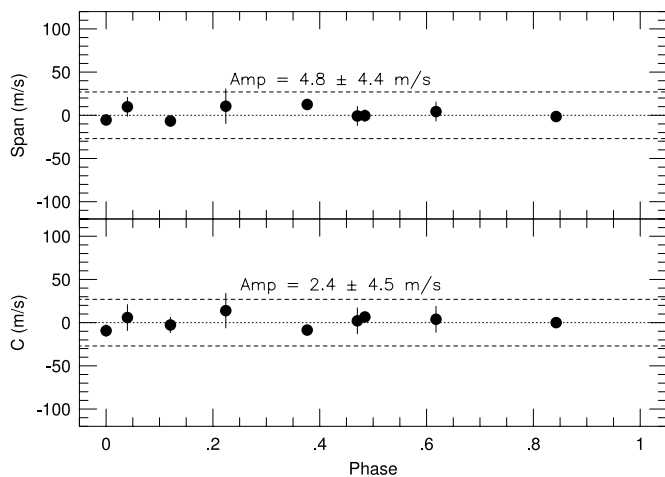
FIG. 5.—Mean bisector span measurements (*top*) and mean bisector curvature (*bottom*) measurements for γ Cep, phased to the planet orbital period. The dotted line marks zero value, and the dashed line represents the extreme values of the RV variations due to the planetary companion.
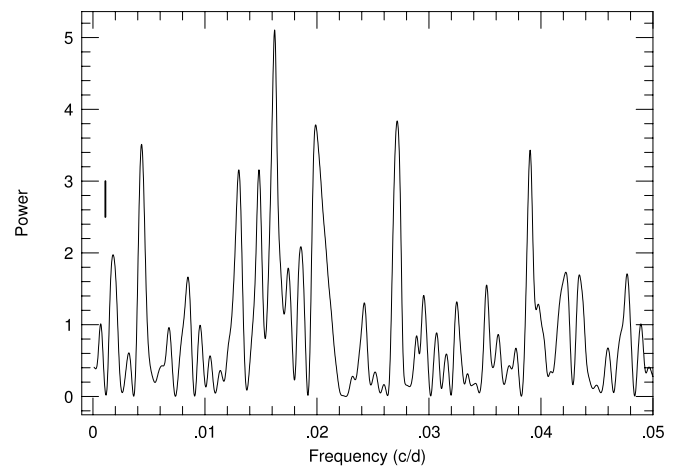

FIG. 7.—Lomb-Scargle periodogram of the *Hipparcos* (daily averages) photometry. The vertical line marks the orbital frequency of the planet.

pulsations were causing the residual RV variations, then this should be evident in the *Hipparcos* photometry.

Figure 6 shows the *Hipparcos* photometry taken from 1989.9 to 1993.2, phased to the planet orbital period. Crosses represent individual measurements, while solid points represent phase-binned averages ($\Delta\phi < 0.05$). Error bars represent the rms scatter of the measurements used for each bin. There are no obvious photometric variations with the planet period, as confirmed by a periodogram analysis of the daily averages of the *Hipparcos* photometry (Fig. 7). A least-squares sine fit to the phased photometric data yields an amplitude of $\Delta V = 0.001 \pm 0.0009$ mag for any possible photometric variations. (A fit to the phase-binned measurements yields $\Delta V = 0.0003$.) The lack of photometric variations in γ Cep is also consistent with the planet hypothesis for the residual RV variations for this star.

4.3. Ca II *Variations*

4.3.1. *S-Index Measurements*

Stellar activity in γ Cep could induce significant periodic centroid shifts in photospheric absorption lines that could be confused for perturbations made by planetary companions (Saar & Donahue 1997; Saar & Fischer 2000; Queloz et al. 2001). For the phase III data an instrumental setup was chosen so as to include the Ca II H and K lines on the detector.

To measure stellar chromospheric activity, the Mount Wilson *S*-index was adopted. This index is defined (e.g., Baliunas et al. 1995) as a quantity proportional to the sum of the flux in 1 Å FWHM triangular bandpasses, centered on the Ca II H and K lines and divided by the sum of the flux in 20 Å bandpasses in the continuum at 3901 and 4001Å (Soderblom, Duncan, & Johnson 1991).

The four quantities to be measured (the two calcium line core fluxes plus the two continuum bandpass fluxes) are spread across three echelle spectral orders that overlap by several Å. In order to be consistent with activity monitoring with our other programs (Paulson et al. 2002), we did not use measurements in the bluemost order, i.e., the continuum region centered on 3901 Å. In addition, we did not measure the Ca II H line (at 3968.47 Å), because the wings of strong Balmer Hϵ feature (at 3970.07 Å) are within the measured Ca II bandpass. This can adversely affect the measurement of the Ca II H line flux. Therefore, we have defined an index $S_{\rm McD}$, which is the ratio of the flux in a 1 Å triangular bandpass centered on the Ca II K line to the flux in a 20 Å bandpass centered on the redward continuum at 4001 Å. Thirty of our program stars (for the MOPS) have previously been measured as part of the Mount Wilson survey (Baliunas et al. 1995; Duncan et al. 1991). We find a linear relationship between our measurements and those of the Mount Wilson survey of the form

$$S_{\rm Mt.\,Wilson} = 0.038(\pm 0.006) + 1.069(\pm 0.040)S_{\rm McD} \,. \quad (1)$$

Both the slope and intercept of the formal fit are within 1 σ of $S_{\rm McD} = S_{\rm Mt.\,Wilson}$. We are thus able to transform our data into a standard Mount Wilson *S*-index scale using equation (1).

FIG. 6.—*Hipparcos* photometry for γ Cep over 1989.9–1993.17, phased to the planet orbital period. The crosses represent the individual measurements, and the solid points represent phased-binned averages. The error bars indicate the rms scatter of values used in computing the binned average.
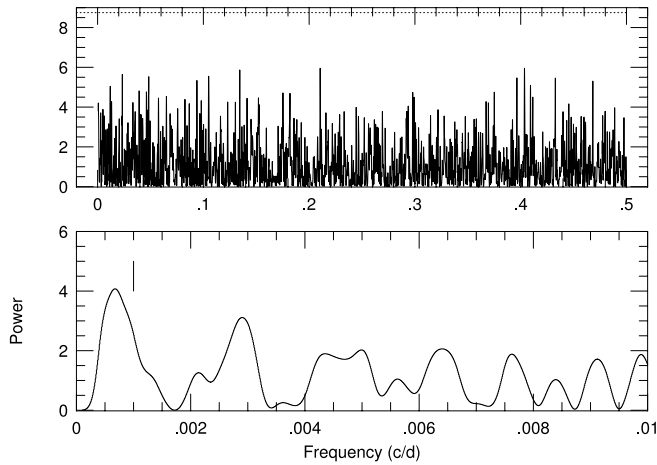
Fig. 8.—Periodogram of the *S*-index measurements using the McDonald phase III data. The vertical line in the lower, expanded-scale plot marks the location of the orbital frequency of the planet. The horizontal dashed line in the top panel indicates an FAP of 1%.

The periodogram of the *S*-index measurements (Fig. 8) shows no significant power at the orbital frequency of the planet. The FAP of the highest peak, assessed using a bootstrap randomization process (Murdoch, Hearnshaw, & Clark 1993; Kürster et al. 1997), is 50%. The lack of variability at the planet period is substantiated by phasing these variations to the 906 day period (Fig. 9). Clearly, no significant sinusoidal variations in this chromospheric index are present. The transformed Ca II K *S*-index for γ Cep is −5.3, which implies a level of magnetic activity less than that of the Sun.

4.3.2. *Analysis of the* Ca II *λ8662 Data from Walker et al.* (*1992*)

A conclusion regarding the planetary nature of the residual RV variations of γ Cep would not be complete without a discussion of the Ca II variations found by Walker et al (1992). Although the McDonald *S*-index measurements do not show evidence for rotational modulation, the Ca II

Fig. 10.—Correlation between the RV and the Ca II λ8662 equivalent width (*top*) and the RV and the *S*-index measurements. A typical error bar is shown in the lower right of the figure.

λ8662 equivalent width measurements (W_λ) of Walker et al. (1992) did show a hint of sinusoidal variations when phased to the planetary orbital period. Although this on its own does not completely refute the existence of a planet, having Ca II variations with the same period would cast more doubt on this hypothesis. For these reasons we made a careful examination of the significance of the Ca II variations reported by Walker et al. (1992).

Figure 10 shows the correlation between the RV and the changes in the Ca II λ8662 equivalent width. The two quantities show no obvious correlations. The correlation coefficient, *r*, is only 0.08, and the probability that the two quantities are not correlated is 0.52. However, there are two obvious outliers in the figure ($|\Delta W_\lambda| > 3\%$). Eliminating these two points increases the correlation coefficient to $r = 0.23$, with a probability of 0.08 that the quantities are uncorrelated. However, this is still not a strong correlation.

The McDonald *S*-index data also do not seem to be correlated to the RV measurements. Figure 11 shows the correlation between the *S*-index and RV measurements from the McDonald data. The correlation coefficient in this

Fig. 9.—*S*-index measurements from the McDonald phase III data phased to the orbital period of the planet. Crosses represent the individual measurements, and solid points represent phased-binned averages. The error bars represent the rms scatter of the data used for the binned averages.
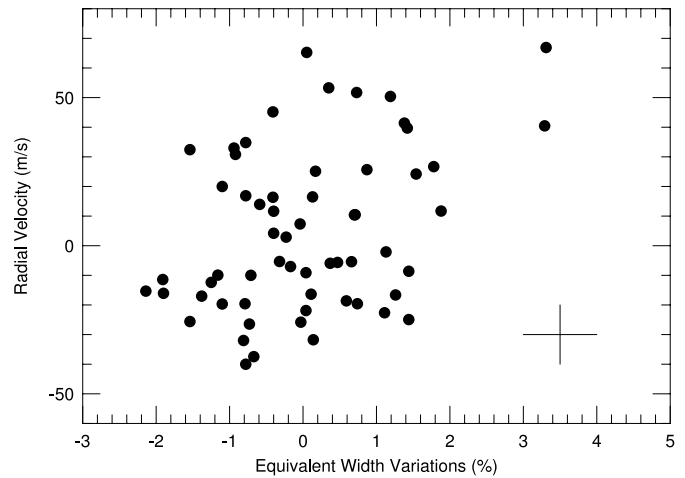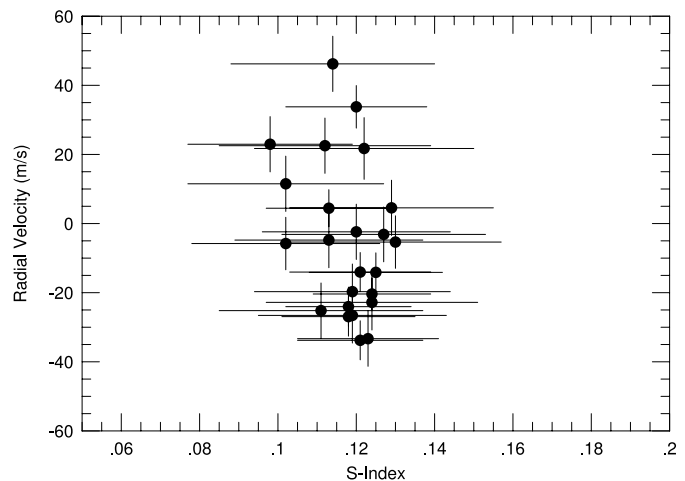

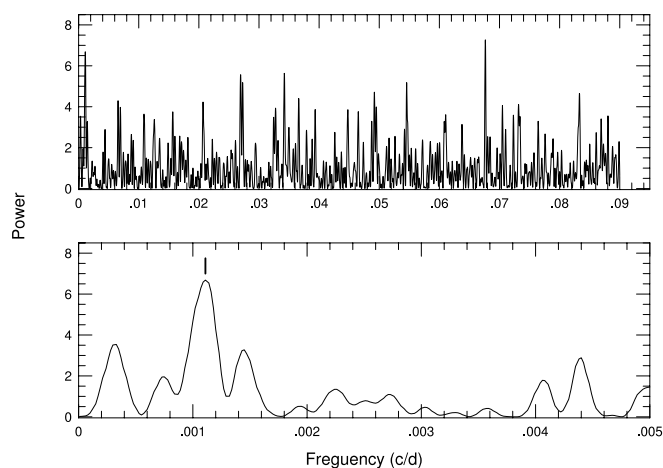Fig. 11.—Correlation between the RV and McDonald Ca II *S*-index measurements measurements.

FIG. 12.—Periodogram of the CFHT Ca II λ8662 equivalent width measurements. The lower panel is an expanded scale near the planet orbital frequency (*vertical line*).

FIG. 13.—*Top*: Lomb-Scargle periodogram for the CHFT Ca II λ8662 measurements over the time span 1981–1986.5. *Bottom*: The same for the time span 1986.5–1992. The vertical line marks the orbital frequency of the planet.

case is $r = -0.3$, and the probability that the two quantities are uncorrelated is 0.13.

Figure 12 shows the Lomb-Scargle periodogram of the variations in the Ca II λ8662 equivalent width measurements of Walker et al. (1992). (There was a clear outlier in the Walker et al. Ca II data with $\Delta EW = -4.3$. This was also evident in Fig. 3 of Walker et al. 1992. This data point was eliminated before performing the periodogram analysis.) Although the most power occurs at a period of ≈15 days (*top panel*), there appears to be significant power at the planet period in the expanded scale in the bottom panel (the vertical line indicates the location of the planet RV frequency). This was the basis on which Walker et al. favored rotational modulation as the cause of the RV variations.

A more detailed examination of the CFHT Ca II λ8662 equivalent width measurements shows that the variation in these are not long-lived and may have no relation to the observed 906 day RV period. We divided the CFHT Ca II data into two data sets, one spanning 1981–1986.5 and the second 1986.5–1992. The division of the data set was taken so as to maximize the power in the long-period variations found in the second set. (Our results do not change substantially if we divide the data set into subsets with equal numbers of points.) This resulted in 21 data points in the first data set and 29 in the second.

Figure 13 shows the periodograms of these two data sets. The 1981–1986.5 set shows no power in the frequency interval 0 cycles day$^{-1} < \nu < 0.01$ cycles day^{-1}. The 1986.5–1992 data set shows significant power but at a frequency corresponding to a period of 781 ± 116 days, significantly less than the planet orbital period. Extending the periodogram to higher frequencies shows that this is the highest peak out to the Nyquist frequency, in contrast to the case for the full data set, in which the low-frequency feature was the second highest peak. A periodogram analysis of the full Ca II data set lowers the Lomb-Scargle power near $\nu = 0.011$ cycles day^{-1} from about 9.0 to 6.7 and increases the period slightly. Unlike the case for the RV data, increasing the number of measurements does not increase the power in the periodogram of the feature of interest. Clearly, this signal is not long-lived.

The statistical significance of this signal was examined using the bootstrap randomization technique. The Ca II
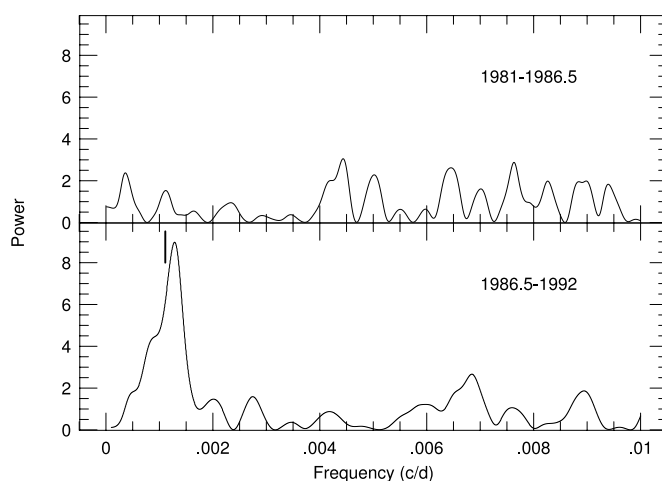
λ8662 equivalent width measurements over the time span 1986.5–1992 were randomly shuffled, keeping the observed times fixed. A periodogram was then computed for each "random" data set. The fraction of the periodograms having power higher than the data periodogram in the range 0.0005 cycles day$^{-1} < \nu < 0.01$ cycles day^{-1} is the FAP that noise would create the detected signal. After 10^5 shuffles there was no instance of a random periodogram having power higher than that found in the data periodogram. The FAP is thus less than 10^{-5}. This signal, in spite of only being present in the data for the last half of the data set, is highly significant.

The period of the Ca II λ8662 measurements is significantly less, by 1 σ, than the residual RV period. Figure 14 shows the phase diagrams of the Ca II λ8662 measurements. In the top panel are the measurements during 1986.5–1992 phased to the 781 day period found in the Ca II data. The middle panel shows the same data, phased to the 906 day residual RV period. Although there are slight sinusoidal
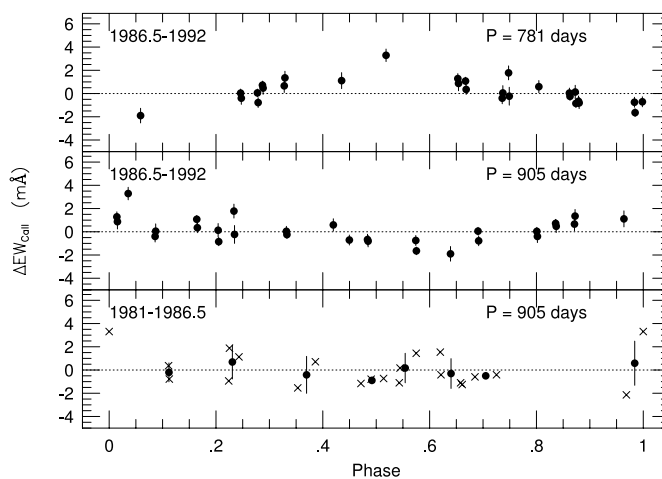

FIG. 14.—The 1986.5–1992 CFHT Ca II measurements phased to the period found in the periodogram analysis (*top*) and the planet period (*middle*). The bottom panel shows the CFHT Ca II equivalent width variations from 1981 to 1986.5 phased to the planet period.

variations when phased to the 906 day period, phasing to the 781 day period produces significantly less scatter. By comparison, the bottom panel shows the Ca II measurements from 1981 to 1986.5, phased to the 906 day period. Crosses represent individual measurements, whereas solid points represent phase-binned averages (the error bar represents the scatter of the data used for each phase bin). There are no significant sinusoidal variations in the 1981–1986.5 data set.

A least-squares sine fit to the the phased Ca II yields an amplitude of 1.67 ± 0.25 mÅ for the dates spanning 1986.5–1992 (1.03 ± 0.25, assuming a 906 day period). For the dates covering 1981–1986.5, the amplitude of the EW_{8662} variations is 0.48 ± 0.33 mÅ. Clearly, there are amplitude variations in the Ca II $\lambda 8662$.

We conclude that the periodic variations in Ca II found by Walker et al. (1992) are not long-lived and were only present during 1986.5–1992. This period was clearly not present in our Ca II S-index measurements spanning 1998–2002. Since the RV variations are unchanged during the entire time span 1981–2002, we do not believe that the 906 day RV period is related to the cause of the Ca II $\lambda 8662$ variability.

4.4. *The Spectral Classification of γ Cep*

One reason that Walker et al. (1992) favored rotational modulation for the residual RV variations was the reclassification of γ Cep as a K0 III. This was based on a visual comparison of the spectrum of γ Cep to those of other K giants (Bohlender et al. 1992). Recently, Fuhrmann (2003) presented an extensive spectral analysis of nearby stars in the galactic disk and halo. Included in this study was γ Cep. Table 7 lists the stellar properties derived by Fuhrmann. Also listed are the *Hipparcos* distance (d_{Hip}) and the distance determined spectroscopically (d_{sp}) using the derived stellar parameters. These distances agree to within 3%, indicating that we can have some confidence in the results of the spectral analysis. Fuhrmann's classification of K1 IV for γ Cep is consistent with the subgiant status for η Cep (K0 IV), which has a comparable effective temperature (4990 K), gravity ($\log g = 3.4$), radius ($4.14\,R_\odot$), and bolometric magnitude ($M_{bol} = 2.3$). The most current and best analysis of γ Cep supports this being a subgiant star.

5. SEARCHING FOR ADDITIONAL COMPANIONS

The long time baseline of RV monitoring of γ Cep and the emergence of several multiple extrasolar planetary

TABLE 7
Stellar Parameters

Parameter	Value
T_{eff}	4888 K
$\log g$	3.33
[Fe/H]	+0.18
M_{bol}	2.14
Mass	$1.59\,M_\odot$
Radius	$4.66\,R_\odot$
d_{Hip}	13.79 pc
d_{sp}	13.39 pc

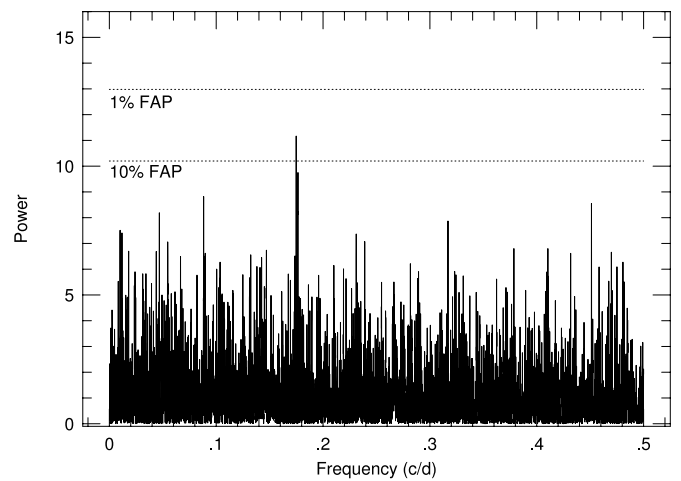Note.—Properties are from Fuhrmann 2003.

Fig. 15.—Lomb-Scargle periodogram of the RV residuals of γ Cep after subtracting the binary and the planetary signal. The horizontal dashed lines show confidence levels with 10% and 1% FAP. Obviously, no additional periodic signal above the noise level is present in the data.

systems from Doppler surveys (e.g., Butler et al. 1999) encouraged us to search for additional companions in this system. For this purpose, we performed a period search within the RV residuals, after subtracting both the binary orbital motion and the first planetary signal.

Figure 15 shows the Lomb-Scargle periodogram of the RV residuals in the period range of 2–7900 days (frequency = 0.00013–0.5 counts day^{-1}). The strongest peak is found at $P \approx 11$ days, but its significance level is very low (FAP is 6.5%). The FAP levels shown in the figure were determined by 10,000 runs of a bootstrap randomization scheme.

It is clear from this analysis that no additional periodic signal above the noise level is present in the RV residuals of γ Cep, and we thus conclude that the 906 day period planet is the only giant planet in this system evident in our data.

6. DISCUSSION

Precise stellar RV measurements of γ Cep from four independent data sets spanning over 20 yr show long-lived, low-amplitude RV variations ($K = 27.5$ m s^{-1}) superposed on the larger RV variations due to the reflex motion caused by a stellar companion. We interpret the low-amplitude, shorter period variations as due to the presence of a planetary companion with $M \sin i = 1.7 M_J$ and an orbital semimajor axis, $a = 2.13$ AU. Our conclusion that these short-period variations are not due to rotation, pulsations, or changes in the convection pattern of the star is based on several facts:

1. The 2.48 yr period has been present for over 20 yr, with no changes in phase or amplitude during this time.
2. No variations with this period are seen in the McDonald Ca II S-index measurements.
3. Spectral line bisector span and curvature measurements for γ Cep are constant to less than 5 m s^{-1} over an orbital cycle of the planet.
4. Contemporaneous *Hipparcos* photometry is constant to less than 0.001 mag over an orbital cycle.
5. The periodic variations in Ca II $\lambda 8662$ found by Walker et al. (1992) were only present during 1986.5–1992

and are thus most likely not associated with the residual RV variability observed for this star.

The CFHT Ca II data do show evidence for long-period variability. Although this signal is weakly detected in the full data set, it is much stronger only in the last half of the data set spanning 1986.5–1992 and is completely absent in the data from 1981 to 1986.5. Furthermore, our *S*-index measurements made during 1997–2003 show no modulation. If rotational modulation were responsible for the residual RV variations, then we would have seen RV amplitude changes. However, the amplitude and phase for the residual RV variations remained constant. It therefore seems unlikely that rotational modulation is the cause of the 906 day period. Furthermore, the best-fit period to the long-term Ca II variations during 1986.5–1992 is 781 ± 116 days, which is significantly less than the 906 day RV period.

γ Cep shows no Ca II modulation during epochs centered on 1994 and 2000 and modulation (781 day period) during a time centered on 1989. This indicates a possible "activity cycle" period of 10–15 yr, much longer than the presumed planet period.

Our spectral line bisector measurements, which are constant, also support our conclusion that we are not seeing rotational modulation. One could argue that the residual RV variations are due to changes in the convection pattern in the star and not due to magnetic structure (plage, spots). For instance, if the ratio of areas of convective, hot rising cells and intergranule, sinking lanes changes with an activity cycle (in this case, with a period of $\sim$900 days), then the amount of convective blue- (red)shift would change periodically resulting in a measured RV signal. If the stellar magnetic fields are strong enough to alter the convection pattern of the star but too weak to cause chromospheric structure, then we would see RV variations without strong variations in the Ca II emission. However, in this case *we should also see changes in the spectral line bisectors*. The lack of significant variability in the spectral line bisectors does not support the hypothesis of a changing convection pattern on the star, or at least changes that can influence the RV measurements.

The inclination angle of the rotation axis can be estimated by comparing the expected equatorial rotational velocity to the projected rotational velocity ($v \sin i$), assuming that 781 days (the period of the Ca II $\lambda 8662$ variations) is the true rotation period of γ Cep. Fuhrmann (2003) estimates a radius $R = 4.66 \, R_\odot$, which gives an equatorial rotational velocity of 4.9 km s^{-1}. We have measured a $v \sin i = 1.5 \pm 1.0$ km s^{-1}, which is consistent to the value determined by Fuhrmann (2003). This yields a $\sin i = 0.5$–0.1. Assuming that the orbital and rotation axes of the star are aligned,

the true mass for the planetary companion to γ Cep is $\approx$3–16M_J.

Given that the 906 day RV variations are due to a substellar companion, the question arises whether this system is stable. After all, both the planet and the stellar companion have modestly eccentric orbits. Preliminary indications are that this system is indeed stable (Dvorak et al. 2003). (The study by Dvorak et al. was made prior to the publication of our paper, and it used preliminary orbital parameters published only in conference abstracts. The stability analysis should be redone using the final parameters and error estimates we have presented here.)

The γ Cep system presents a very interesting system for the study of planet formation. Planets have been found around host stars that are in binary systems, but these are widely separated pairs, so the presence of the stellar companion may not have an influence on the planet formation around one of the stars. The γ Cep binary is the shortest period binary for which a planetary companion has been found in orbit around one of the components. This implies that even in such a relatively close binary the presence of the stellar companion does not hinder the process of planet formation.

One final comment—RV surveys have had stunning success at finding planets in orbit around other stars. Yet this is still an indirect detection method, with the disadvantage that various stellar phenomena can mimic a planetary signal. RV searches for extrasolar planets are, and should continue to be, a careful process, with many candidates undergoing the painstaking process of confirmation. Several extrasolar planet candidates have a proved to be due to stellar phenomena (Queloz et al. 2001; Butler et al. 2002), and more false detections will undoubtedly be uncovered in the future. Likewise, RV variations that were initially attributed to stellar phenomena in the past may ultimately prove to be due to a planetary companion, as is apparently the case for γ Cep. RV searches for extrasolar planets must be accompanied by careful studies of the host star and the measurement of various photometric and spectroscopic (Ca II emission, line shapes) quantities. These measurements are important, for they could have confirmed the planet around γ Cep 7 yr prior to the discovery of 51 Peg b.

REFERENCES

Baliunas, S. L., et al. 1995, ApJ, 438, 269
Bohlender, D. A., Irwin, A. W., Yang, S. L. S., & Walker, G. A. H. 1992, PASP, 104, 1152
Brown, T. M., Kotak, R., Horner, S. D., Kennelly, E. J., Korzennik, S., Nisenson, P., & Noyes, R. W. 1998, ApJS, 117, 563
Butler, R. P., Marcy, G. W., Fischer, D. A., Brown, T. M., Contos, A. R., Korzennik, S. G., Nisenson, P., & Noyes, R. W. 1999, ApJ, 526, 916
Butler, R. P., Marcy, G. W., Williams, E., McCarthy, C., Dosanjh, P., & Vogt, S. S. 1996, PASP, 108, 500
Butler, R. P., Tinney, C. G., Marcy, G. W., Jones, H. R. A., Penny, A. J., & Apps, K. 2001, ApJ, 555, 410
Butler, R. P., et al. 2002, ApJ, 578, 565
Campbell, B., & Walker, G. A. H. 1979, PASP, 91, 540
Campbell, B., Walker, G. A. H., & Yang, S. 1988, ApJ, 331, 902
Cochran, W. D., & Hatzes, A. P. 2003, in IAU Symp. 202, Planetary Systems in the Universe: Observation, Formation, and Evolution, ed. A. J. Penny, P. Artymowicz, A.-M. Lagrange, & S. S. Russell (San Francisco: ASP), in press
Duncan, D. K., et al. 1991, ApJS, 76, 383
Dvorak, R., Pilat-Lohinger, E., Funk, B., & Freistetter, F. 2003, A&A, 398, L1
Endl, M., Kürster, M., & Els, S. 2000, A&A, 362, 585
Frink, S., Mitchell, D. S., Quirenback, A., Fischer, D. A., Marcy, G. W., & Butler, R. P. 2002, ApJ, 576, 478
Fuhrmann, K. 2003, Astron. Nachr., in press
Griffin, R., & Griffin, R. 1973, MNRAS, 162, 243
Griffin, R. F., Carquillat, J.-M., & Ginestet, N. 2002, Observatory, 122, 90
Hatzes, A. P. 1996, PASP, 108, 839

Hatzes, A. P. 2002, Astron. Nachr., 323, 392
Hatzes, A. P., & Cochran, W. D. 1993, ApJ, 413, 339
Hatzes, A. P., Cochran, W. D., & Bakker, E. J. 1998a, Nature, 391, 154
————. 1998b, ApJ, 508, 380
Hatzes, A.. P., Cochran, W. D., & Johns-Krull, C. M. 1997, ApJ, 478, 374
Jefferys, W., Fitzpatrick, J., & McArthur, B. 1988, Celest. Mech., 41, 39
Koch, A., & Wohl, H. 1984, A&A, 134, 134
Kürster, M., Schmitt, J. H. M. M., Cutispoto, G., & Dennerl, K. 1997, A&A, 320, 831
Libbrecht, K. G. 1988, ApJ, 330, L51
Lomb, N. R. 1976, Ap&SS, 39, 447
McArthur, B., Jefferys, W., & McCartney, J. 1994, BAAS, 26, 900
Murdoch, K. A., Hearnshaw, J. B., & Clark, M. 1993, ApJ, 413, 349
Paulson, D. B., Saar, S. H., Cochran, W. D., & Hatzes, A. P. 2002, AJ, 124, 572
Perryman, M. A. C., et al. 1997, A&A, 323, L49

Queloz, D., et al. 2001, A&A, 379, 279
Saar, S. H., & Donahue, R. A. 1997, ApJ, 485, 319
Saar, S. H., & Fischer, D. 2000, ApJ, 534, L105
Scargle, J. D. 1982, ApJ, 263, 835
Setiawan, J., et al. 2003, A&A, 398, L19
Soderblom, D. R., Duncan, D. K, & Johnson, D. R. H. 1991, ApJ, 375, 722
Tull, R. G., MacQueen, P. J., Sneden, C., & Lambert, D. L. 1995, PASP, 107, 251
Valenti, J. A., Butler, R. P., & Marcy, G. W. 1995, PASP, 107, 966
Walker, G. A. H., Bohlender, D. A., Walker, A. R., Irwin, A. W., Yang, S. L. S., & Larson, A. 1992, ApJ, 396, L91
Walker, G. A. H., Yang, S., Campbell, B., & Irwin, A. W. 1989, ApJ, 343, L21
Walker, G. A. H., Walker, A. R., Irwin, A. W., Larson, A. M., Yang, S. L. S., & Richardson, D. C. 1995, Icarus, 116, 359